Multi-field Coupling of Photothermal and Magnetism for Boosting the Electrocatalytic Hydrogen Evolution Reaction Performance

Chong Liu[1], Lianqing Yu*[1], Nannan Chen[1], Yichao Huang*[1], Yaping Zhang[2], Haifeng Zhu[2]

1. State Key Laboratory of Chemical Safety, Shandong Key Laboratory of Intelligent Energy Materials, School of Materials Science and Engineering, China University of Petroleum (East China), Qingdao, Shandong, 266580, P. R. China

2. College of Science, China University of Petroleum (East China), Qingdao 266580 China.

*Corresponding author Lianqing Yu Email: *iyy2000@163.com*

Yichao Huang Email: yichaoh@upc.edu.cn

Supplementary Methods

Chemicals and materials

Sodium molybdate (VI) dihydrate ($Na_2MoO_4 \cdot 2H_2O$), thiourea (CH_4N_2S), ferric chloride hexahydrate ($FeCl_3 \cdot 6H_2O$), cobalt nitrate hexahydrate (II) ($Co(NO_3)_2 \cdot 6H_2O$), sodium hydroxide (NaOH), and ethanol (C_2H_5OH) were purchased from Aladdin company, (Shanghai, China). The above chemicals were used as received.

Materials characterization

The crystalline structures and elemental composition of the sample were determined by X-ray diffraction (XRD) using Cu Kα radiation. The morphologies and chemical composition were investigated by scanning electron microscopy (SEM, S-4800, Hitachi) and transmission electron microscopy (TEM, JEM-2100, Japan) coupled with EDS-mapping. X-ray photoelectron spectroscopy (XPS) measurements were performed on a Thermo Scientific K-Alpha XPS spectrometer using an Al Kα X-ray

source. All of the binding energies were calibrated according to the reference energy of C 1s (C 1s = 284.5 eV). The optical performance of the products was assessed using UV/Vis diffuse reflectance spectroscopy (DRS).

Electrochemical characterization

All electrochemical tests were conducted using an electrochemical workstation (CHI 760E, Chenhua, Shanghai) in a standard three-electrode set-up at room temperature. A graphite rod and a saturated Ag/AgCl electrode were employed as the counter and reference electrodes, respectively, while the prepared electrocatalysts were employed directly as the working electrodes. Water splitting experiments were performed in 1 M KOH solution at room temperature. For the HER test, the linear sweep voltammograms (LSV) were recorded from -1.6 V to 0 V at a scan rate of 5 $mV \cdot s^{-1}$. The potentials were converted to the RHE scale using the following Nernst equation: (E(RHE) = E(Ag/AgCl) + 0.059 pH + 0.197). The electrochemical impedance spectroscopy (EIS) was performed over a frequency range of 100 kHz to 0.01 Hz, with the applied potential being an open circuit potential. To estimate the electrochemically active surface area (ECSA), the C_{dl} values were obtained by collecting CVs measurements performed at various scan rates of 20, 40, 60, 80, 100 and 120 $mV \cdot s^{-1}$ under the potential window of -0.9 to -0.7 V *vs.* RHE. A long-term stability test was carried out with a chronopotentiometric (CP) technique in 1.0 M KOH electrolyte with the current density of 10 $mA \cdot cm^{-2}$.

Computational Method

All first-principle calculations were conducted using density functional theory (DFT) within the Cambridge Sequential Total Energy Package (CASTEP) module of Materials Studio. The generalized gradient approximation (GGA) of Perdew-Burke-Ernzerhof (PBE) scheme was adopted to calculate the exchange correlation energies. A cut-off energy of 450 eV was used for the plane-wave basis set. A 3 × 3 × 1 Monkhorst–Pack grid was adopted to sample the Brillouin zone. The convergence thresholds for

energy and Hellmann–Feynman forces were set to 10^{-5} eV and 0.01 eV·Å^{-1}, respectively. The electronic self-consistent field (SCF) tolerance was set to 1.0×10^{-6} eV per atom.

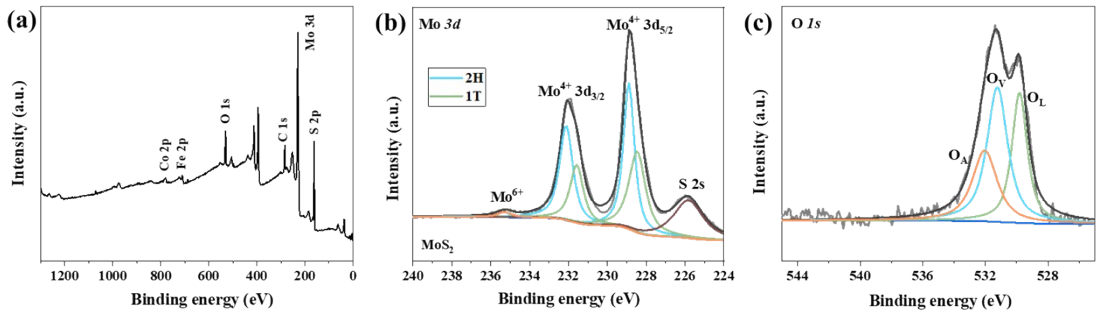

Fig. S1. (a) XPS total survey of $CoFe_2O_4/MoS_2$. High-resolution XPS spectra (b) Mo 3d and (c) O 1s of $CoFe_2O_4/MoS_2$.

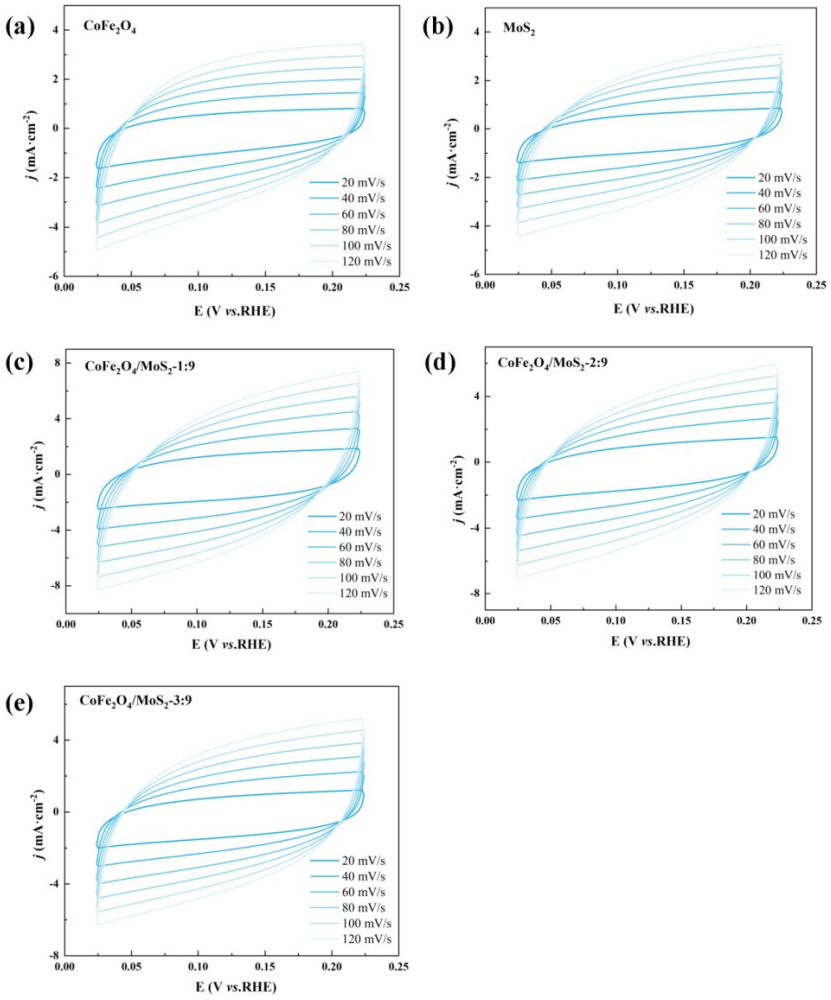

Fig. S2. Cyclic voltammetry curves of $CoFe_2O_4$ (a), MoS_2 (b), $CoFe_2O_4/MoS_2$-1:9 (c), $CoFe_2O_4/MoS_2$-2:9 (d), and $CoFe_2O_4/MoS_2$-3:9 (e) at different scanning rates.

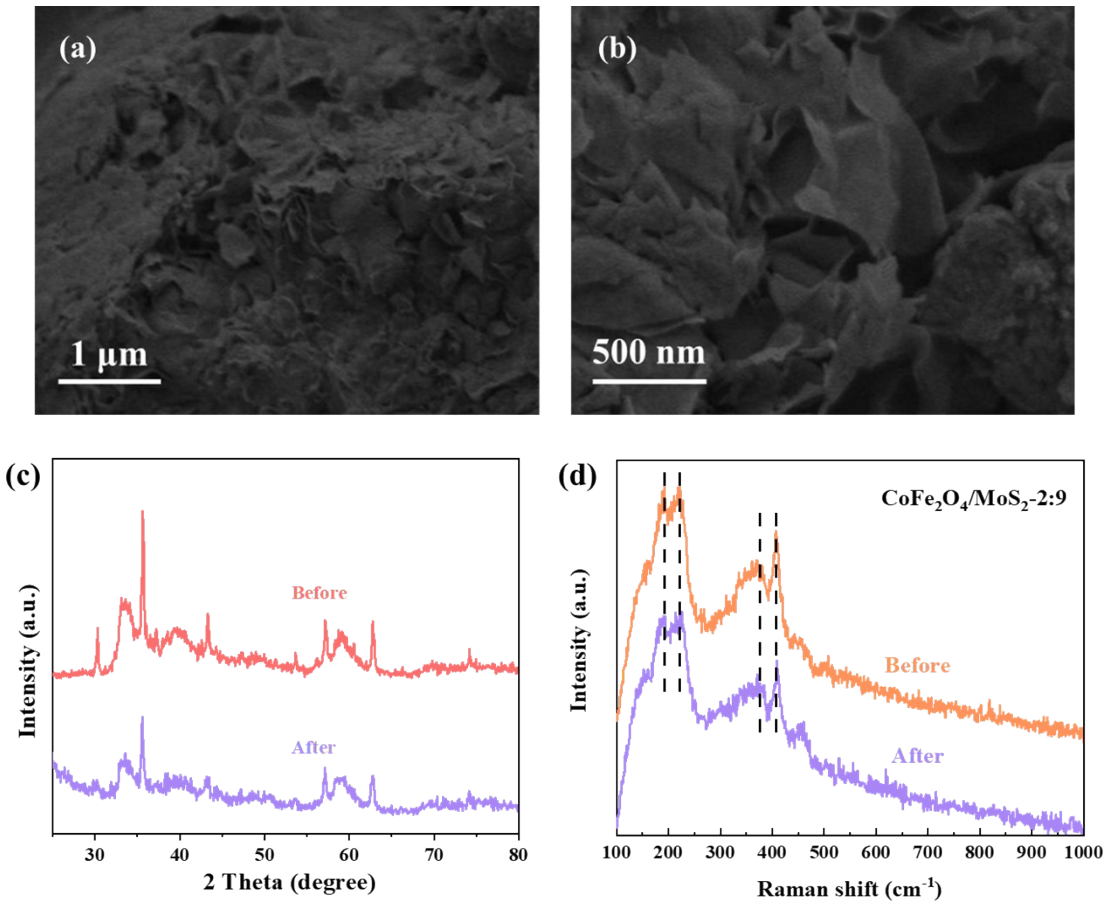

Fig. S3. (a-b) SEM images, (c) XRD patterns and (d) Raman spectra of $CoFe_2O_4/MoS_2$-2:9 after stability tests.

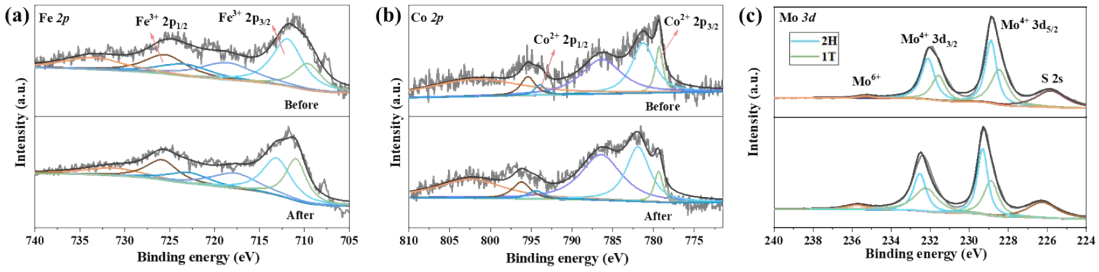

Fig. S4. High-resolution XPS spectra (a) Fe 2p, (b) Co 2p and (c) Mo 3d of $CoFe_2O_4/MoS_2$ before and after stability tests.

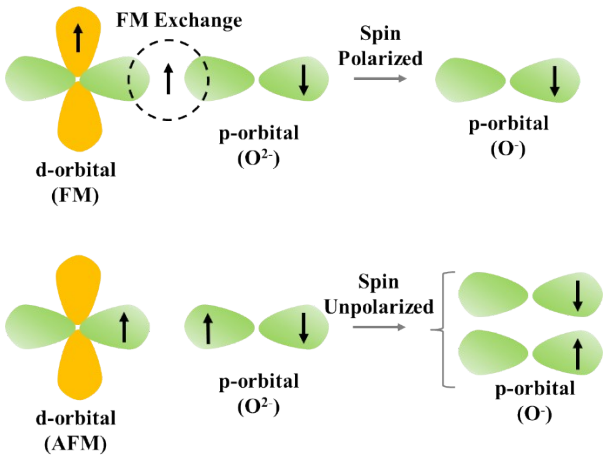

Fig. S5. Schematic diagram of spin electron transfer in catalyst.

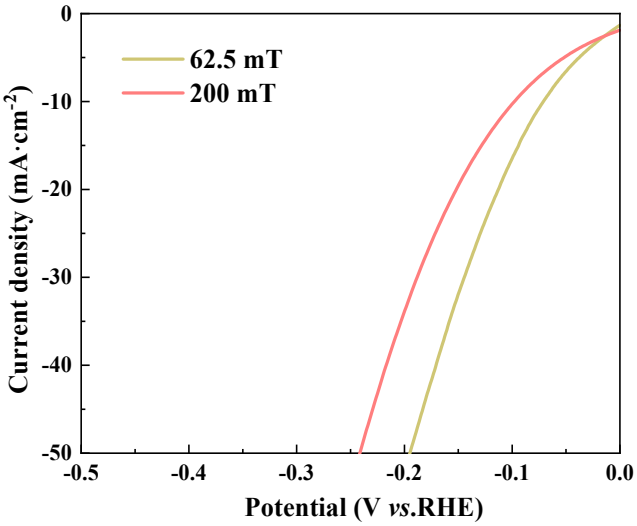

Fig. S6. HER polarization curves of $CoFe_2O_4/MoS_2$-2:9 under magnetic field of 62.5 and 200 mT.

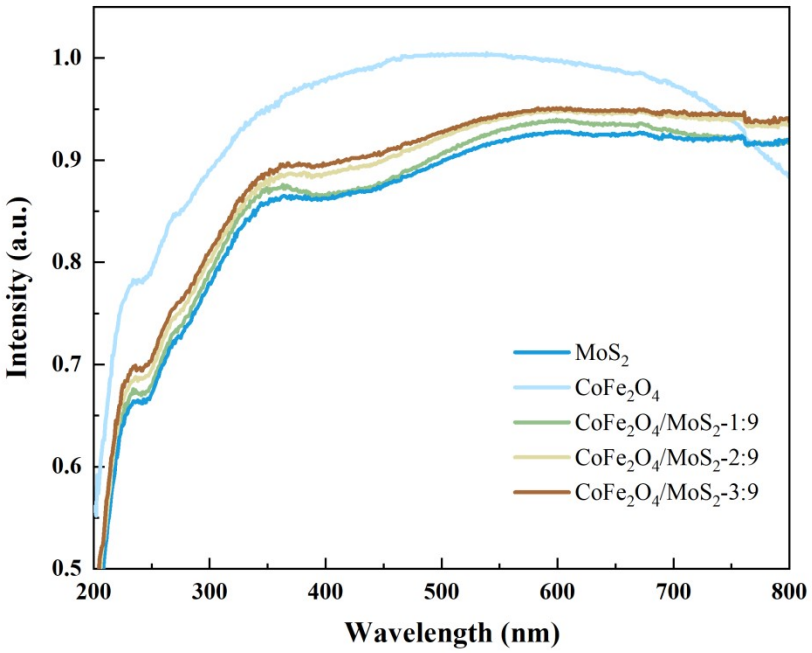

Fig. S7. UV-vis-NIR DRS spectra.

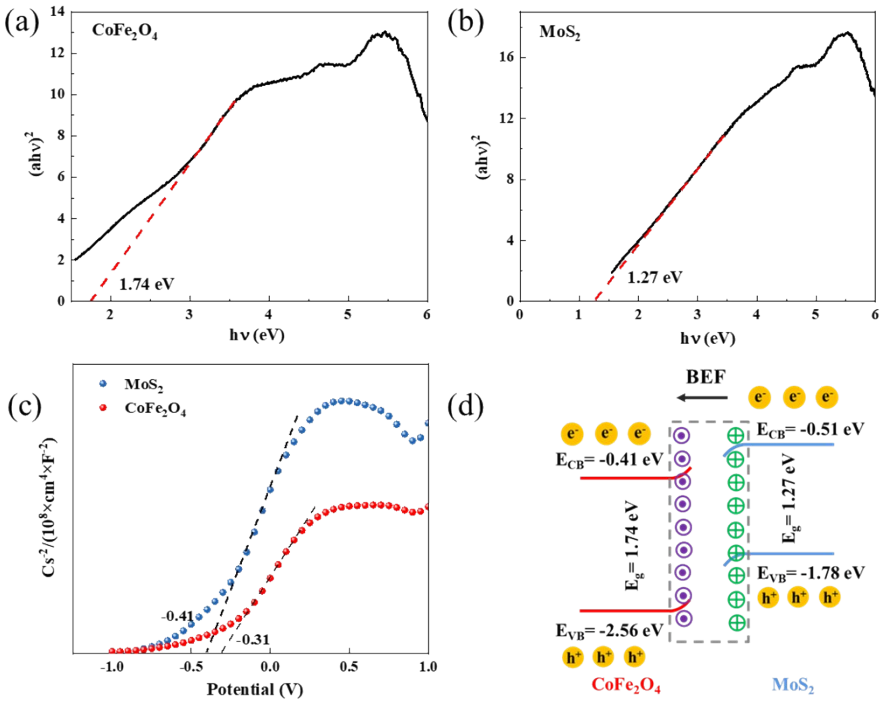

Fig. S8. Band-gap energies for (a) $CoFe_2O_4$ and (b) MoS_2. (c) Mott-Schottky plots. (d) Schematic representation of the charge transfer process

Table S1 Values of resistance (R_s), and charge transfer resistance (R_{ct}) obtained after fitting the Nyquist plots determined on different samples.

Electrocatalysts	**R_s (Ω)**	**R_{ct} (Ω)**
MoS_2	1.181	2.525
$CoFe_2O_4$	1.491	1.204
$CoFe_2O_4/MoS_2$-1:9	1.428	0.466
$CoFe_2O_4/MoS_2$-2:9	1.744	0.231
$CoFe_2O_4/MoS_2$-3:9	1.374	0.563

Table S2. Summary of several recently representative reported HER electrocatalysts employed in acidic and alkaline electrolytes.

Catalyst	Electrolyte	Overpotemtial (mV)	Tafel slope ($mV \cdot dec^{-1}$)	Reference
$CoFe_2O_4/MoS_2$-2:9	1M KOH	64	98	This work
1T-MoS_2/NiS_2	1M KOH	116	72	[1]
R-MoS_2@NF	1M KOH	71	100	[2]
Co_3O_4/MoS_2	1M KOH	205 mV at 20 $mA \cdot cm^{-2}$	98	[3]
meso-Fe-$MoS_2/CoMo_2S_4$	1M KOH	122	90	[4]
$MoS_2/NiFe_2O_4$	1M KOH	190	/	
FeMn-LDH/MoS_2	1M KOH	120	112	[5]
Co_9S_8/MoS_2	0.5 M H_2SO_4	233	118	[6]
MCM@MoS_2–Ni	0.5 M H_2SO_4	161	179	[7]

References

1. X. Chen, Z. Wang, Y. Wei, X. Zhang, Q. Zhang, L. Gu, L. Zhang, N. Yang and R. Yu, *Angew. Chem., Int. Ed.*, 2019, **58**, 17621-17624.
2. M. A. R. Anjum, H. Y. Jeong, M. H. Lee, H. S. Shin and J. S. Lee, *Adv. Mater.*, 2018, **30**, 1707105.
3. A. Muthurasu, V. Maruthapandian and H. Y. Kim, *Appl. Catal., B*, 2019, **248**, 202-210.
4. Y. Guo, J. Tang, J. Henzie, B. Jiang, W. Xia, T. Chen, Y. Bando, Y.-M. Kang, M. S. A. Hossain, Y. Sugahara and Y. Yamauchi, *ACS Nano*, 2020, **14**, 4141-4152.
5. S. Kumar, S. Raju, S. Marappa, M. S, V. D R, D. M and B. H, *ACS Appl. Energy Mater.*, 2024, **7**, 9872-9881.
6. T.-T. Chen, R. Wang, L.-K. Li, Z.-J. Li and S.-Q. Zang, *J. Energy Chem.*, 2020, **44**, 90-96.
7. H. Zhang, L. Yu, T. Chen, W. Zhou and X. W. Lou, *Adv. Funct. Mater.*, 2018, **28**, 1807086.